

Fig. S1 AFM images of the GCE/CS-SCS- $\alpha$ -CD (a) surfaces and of the GCE/CS-SCS- $\gamma$ -CD surface.

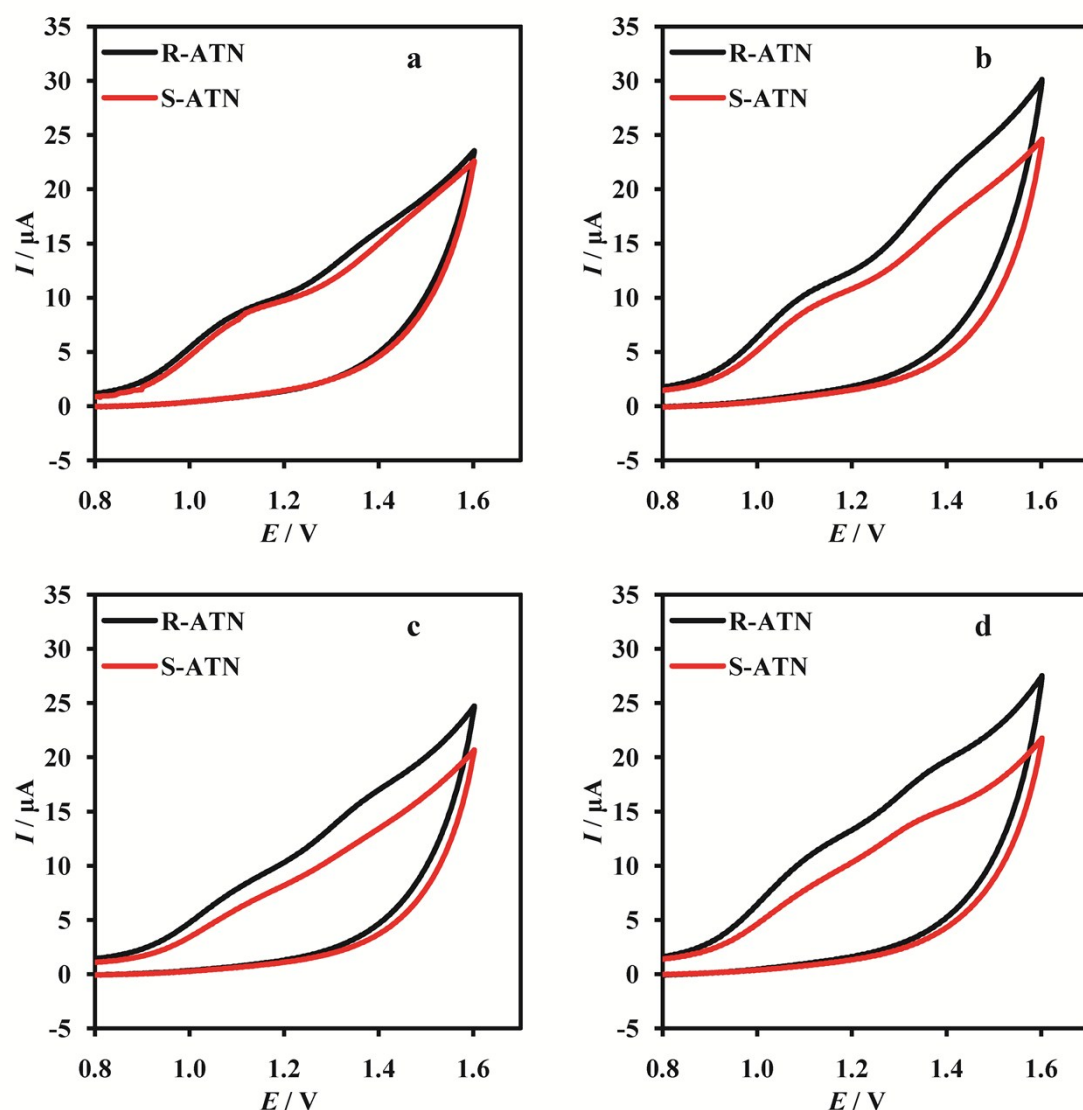


Fig. S2.CVs of 0.5 mM solutions of R- and S-ATN enantiomers in a borate buffer solution of pH 9.18 on GCE/CS-SCS (a), GCE/CS-SCS- $\alpha$ -CD (b), GCE/CS-SCS- $\beta$ -CD (c)and GCE/CS-SCS- $\gamma$ -CD (d) at 100 mVs<sup>-1</sup>.

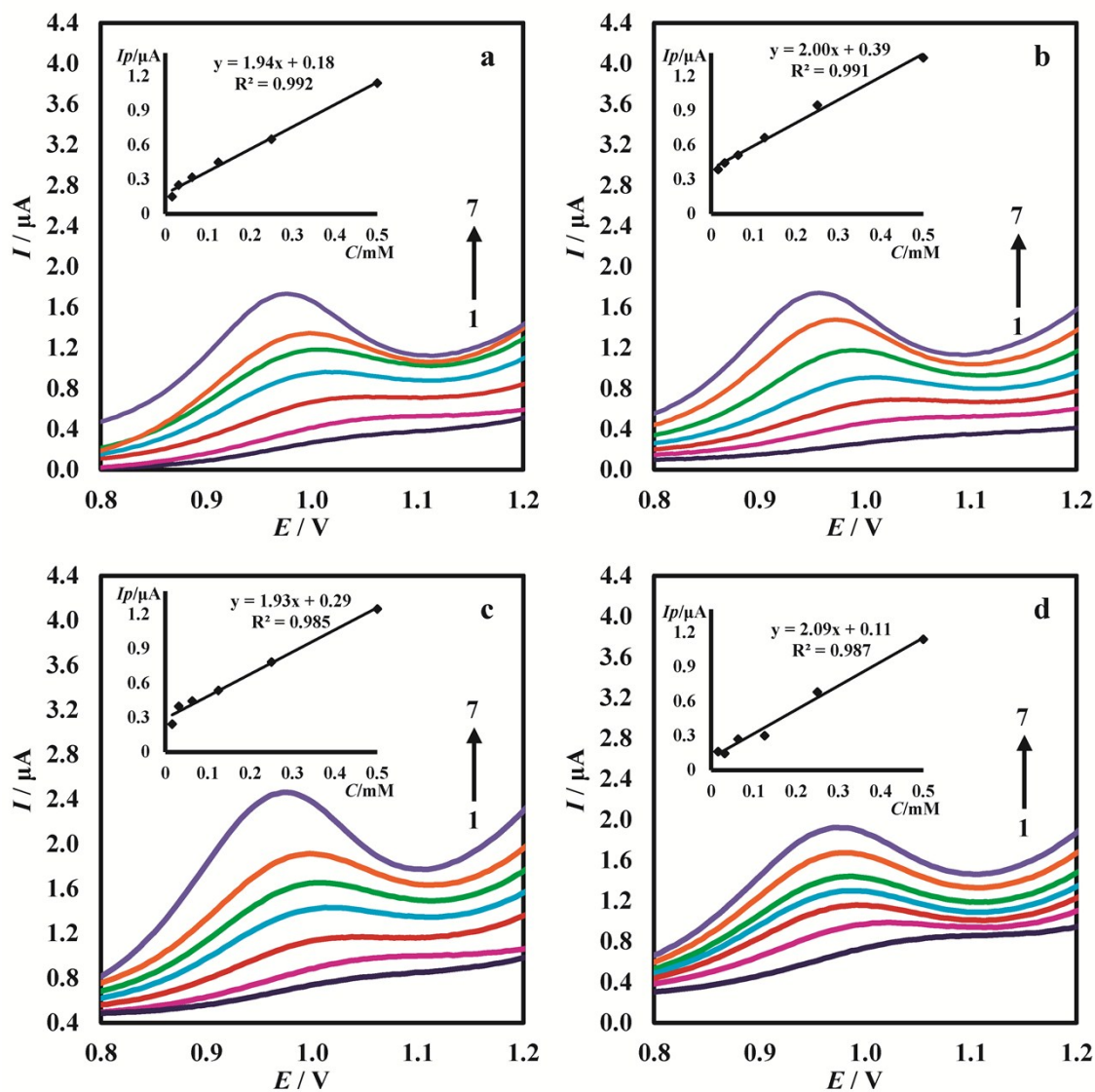


Fig. S3.DPVs of GCE/CS-SCS (a), GCE/CS-SCS- $\alpha$ -CD (b), GCE/CS-SCS- $\beta$ -CD (c) and GCE/CS-SCS- $\gamma$ -CD (d) at  $20 \text{ mVs}^{-1}$  for different concentrations of R-ATN: 0.008 (1), 0.016 (2), 0.031 (3), 0.062 (4), 0.125 (5), 0.25 (6), 0.5 (7) mM in a borate buffer solution of pH 9.18. Insets: corresponding calibration plots.

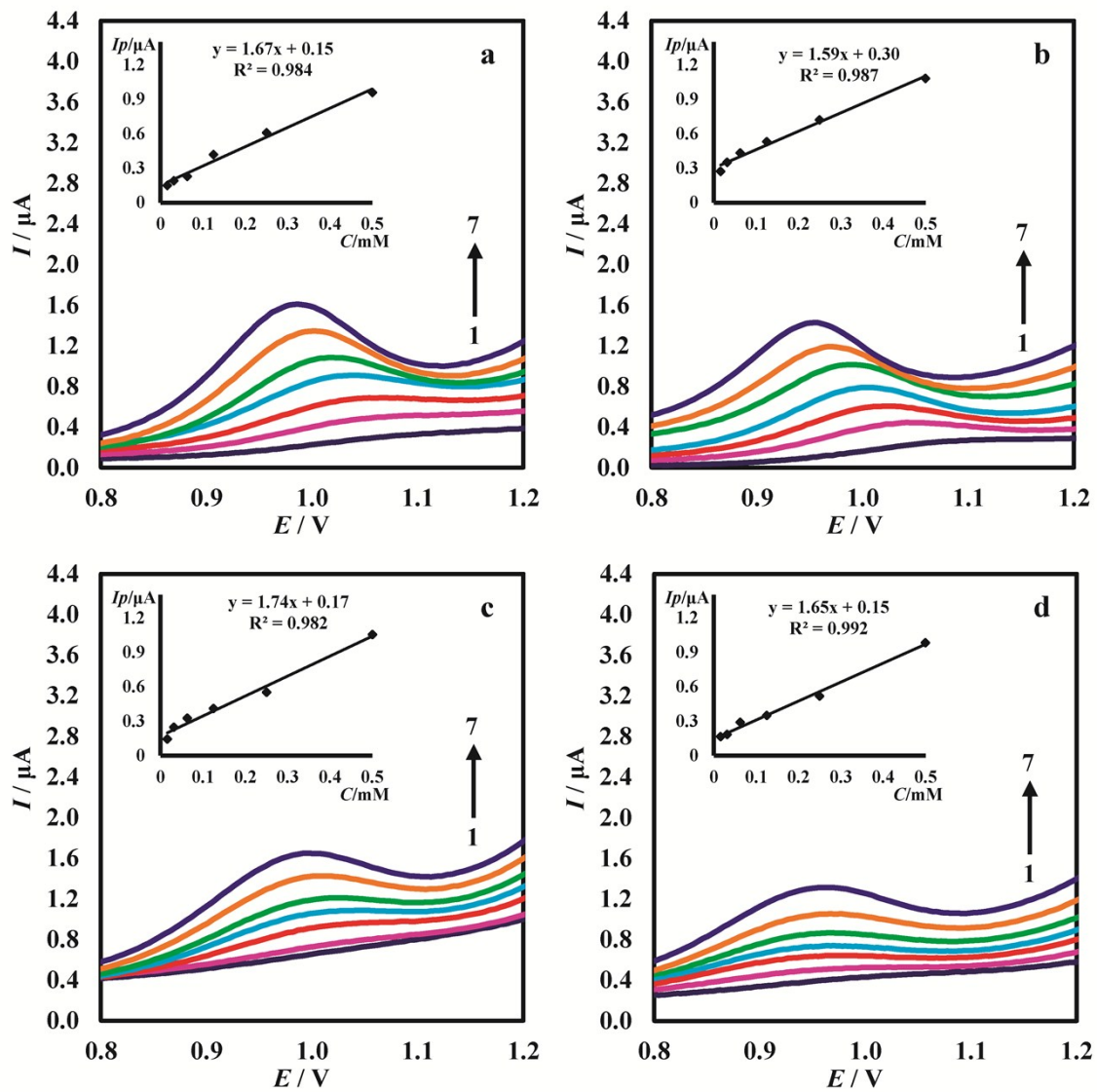


Fig. S4.DPVs of GCE/CS-SCS (a), GCE/CS-SCS- $\alpha$ -CD (b), GCE/CS-SCS- $\beta$ -CD (c) and GCE/CS-SCS- $\gamma$ -CD (d) at  $20 \text{ mVs}^{-1}$  for different concentrations of S-ATN: 0.008 (1), 0.016 (2), 0.031 (3), 0.062 (4), 0.125 (5), 0.25 (6), 0.5 (7) mM in a borate buffer solution of pH 9.18. Insets: corresponding calibration plots.